Oligoesters Based on Poly(*p*-alkoxycinnamate) and Poly(pentaethylene glycol cinnamate) as Potential UV Filters

S. Sasiwilaskorn,[1,2] P. Klinubol,[3] A. Tachaprutinun,[3] T. Udomsup,[3] S. P. Wanichwecharungruang[1,3]

[1]*Program of Petrochemistry and Polymer Science, Faculty of Science, Chulalongkorn University, Bangkok 10330, Thailand*
[2]*Science and Technology Division, Nong Khai Campus, Khon Kaen University, Nong Khai 43000, Thailand*
[3]*Sensor Research Unit, Department of Chemistry, Faculty of Science, Chulalongkorn University, Bangkok 10330, Thailand*

Received 16 September 2007; accepted 20 February 2008
DOI 10.1002/app.28335
Published online 2 June 2008 in Wiley InterScience (www.interscience.wiley.com).

ABSTRACT: Four solid UV-absorptive oligomers—poly(*p*-ethoxycinnamate) (**P2**), poly(*p*-propoxycinnamate) (**P3**), poly(*p*-hexyloxycinnamate) (**P6**), and poly(*p*-undecyloxycinnamate) (**P11**)—were condensation polymerized from *p*-(2-hydroxy-ethoxy) cinnamic acid, *p*-(3-hydroxy-propoxy) cinnamic acid, *p*-(6-hydroxy-hexyloxy) cinnamic acid, and *p*-(11-hydroxy-undecyloxy) cinnamic acid, respectively. The liquid UV-absorptive oligomer, poly(pentaethylene glycol cinnamate) (PPGC), was synthesized through the copolymerization between *p*-hydroxycinnamic acid and pentaethylene glycol ditosylate. Molecular weights of all five oligomers were in the range of 1600–5500. Absorption profiles of all synthesized polymers indicated UVB absorption characteristics. Upon UVB exposure, *trans* to *cis* photoisomerization of all five oligomers was observed, leading to the decrease in their UVB absorption efficiency. No transdermal penetration across a baby mouse skin (*Mus musculus* Linn.) was detected for the five synthesized oligomers, while the penetration of the standard UVB filter, 2-ethylhexyl-*p*-methoxycinnamate, through the same skin could be clearly observed. In addition, PPGC, a yellowish water immiscible liquid, showed good solubility in various organic solvents and silicone fluids. PPGC and **P3** could be induced into water dispersible nanoparticles using solvent displacement technique. © 2008 Wiley Periodicals, Inc. J Appl Polym Sci 109: 3502–3510, 2008

Key words: alkoxycinnamate; UV filter; poly(pentaethylene glycol cinnamate); nanoparticles

INTRODUCTION

Long-term exposure to UV radiation on normal human skin leads to direct cellular damage and immunosuppression, resulting in photoaging, mutations, and carcinogenesis.[1,2] UVB (280–315 nm) can interact directly with DNA bases and cause DNA lesions, particularly cyclobutane pyrimidine dimers (CPDs) and pyrimidine (6–4) pyrimidone photoproducts.[3,4] UVA Radiation produces not only the oxidative DNA damage through 8-oxo-7,8-dihydro-2′-deoxyguanosine,[5] but the radiation also induces CPDs formation probably via a triplet energy transfer photosensitization mechanism.[6] Therefore, sunscreen use has become widely practiced. Esters of *p*-methoxycinnamic acid are among the popular UVB screening compounds used in various cosmetic formulations. The most popularly-used derivative in this group is the 2-ethylhexyl *p*-methoxycinnamate (EHMC), which possesses a high molar absorption coefficient (ε), $\sim$ 22,000–24,000M^{-1} cm^{-1}, and shows only a few allergic reactions to human skin.[7,8] Nevertheless, transdermal permeation of the compound into the human body has been reported.[9,10] In fact, transdermal penetrations of many sunscreens have been demonstrated.[11,12] Transdermal absorption of the UV filter directly decreases the UV screening efficiency of the products. Attempts to increase the skin accumulation of UV absorbers include incorporations of the UV filters into delivery systems[13,14] and the alteration of existing formulations.[15] In addition, a few novel polymeric sunscreens have recently been reported. For example, grafting of the UV-absorptive cinnamoyl moieties onto polysaccharide backbone[16] and polysiloxane backbone[17] were carried out to obtain polysaccharide cinnamic acid derivatives and cinnamate-grafted silicone fluid with UV absorbing property, respectively. It should be stated here that, although there are many other investigations on cinnamate polymeric materials, most of them involve

Correspondence to: S. P. Wanichwecharungruang (psupason@chula.ac.th).

Contract grant sponsor: Thailand Research Fund, Office of Commission for Higher Education.

high molecular weight polymers used in optical and electrooptical applications.[18,19] In such applications, UV absorption property of the cinnamate moieties was not the main concern, their crosslinked liquid crystal and chiral photoisomerization properties were more important. In addition to cinnamate polymeric material, polymeric sunscreens based on other UV-absorptive functionalities were also reported.[20–22] Skin penetration of the polymeric UV filters could be avoided due to the presumed low diffusion of large polymers through skin over a limited period of time. In this study, we report the synthesis of UV-absorptive oligomers, poly(*p*-alkoxycinnamates) and poly (pentaethylene glycol cinnamate). The materials have similar UV-absorptive functionalities to EHMC. Their UV absorption properties and photostability were determined and their transdermal absorptions through baby mice skin were compared with EHMC.

EXPERIMENTAL

Solvents used in the synthesis and the spectroscopic works were of reagent or analytical grades purchased from Labscan (Bangkok, Thailand). *p*-Hydroxycinnamic acid, 2-bromoethanol, 3-bromo-1-propanol, 6-bromo-1-hexanol, 11-bromo-1-undecanol, 1-(3-dimethylaminopropyl)-3-ethylcarbodiimide hydrochloride (EDCI), and 1-hydroxy-benzotriazole (HOBt) were purchased from Acros (Geel, Belgium). Potassium carbonate, *p*-toluene sulfonic acid, Amberlyst-15, and pentaethylene glycol ditosylate were purchased from Fluka Chemical Company (Buchs, Switzerland). *N*,*N*′-dicyclohexylcarbodiimide (DCC) was purchased from Merck (Darmstad, Germany). Standard EHMC was a kind gift from Merck Thailand (Bangkok, Thailand).

The ^{1}H and ^{13}C NMR spectra were obtained in deuterated chloroform ($CDCl_3$) or deuterated dimethylsulfoxide (DMSO-d_6) with tetramethylsilane (TMS) as an internal reference using a Varian Mercury spectrometer that operated at 400.00 MHz for ^{1}H and 100.00 MHz for ^{13}C nuclei (Varian Company, Palo Alto, CA). The IR spectra were recorded on a Nicolet Fourier transform infrared spectrophotometer: Impact 410 (Nicolet Instrument Technologies, Madison, WI). Molecular weights were determined by gel permeation chromatography (GPC) using a Waters Styragel HR low molecular weight column and waters 600E multisolvent delivery system (Waters, MA). UV Spectra were obtained with the aid of an HP 8453 UV/VIS spectrophotometer (Agilent Technologies, CA) using a quartz cell with a 1-cm path length. The mass spectra of the synthesized monomers were recorded on a Micromass Quatto Micro API ESCi (Waters, MA) using negative electrospray ionization. The mass spectra of the oligomers were recorded on an Ultraflex MALDI-TOF mass spectrometer (Bruker Daltonics, Bremen, Germany). Melting points were determined with a Stuart Scientific Melting Point SMP 1 (Bibby Sterilin, Staffordshire, UK). Broadband UVB (280–320 nm) was generated by FSX24T12/UVB/HO lamp (National Biological, Twinsburg, OH). UV Irradiance was measured using UVB-500C power meters (National Biological, Twinsburg, OH). Thermogram of each sample was acquired at 0–380°C under nitrogen with a scanning rate of 20°C/min using a differential scanning calorimetry: DSC 204 (Netzsch Group, Selb, Germany). Scanning electron micrographs (SEM) were obtained using JEM-6400 (Jeol, Japan). A drop of the nanoparticle suspension (2 mg/mL) was placed on a glass slide and dried over night. After mounting the slide on aluminum pin, the sample was coated with a gold layer under vacuum at 10 kV for 90 s. Atomic force microscopy (AFM) image of a sample was aquired in a tapping mode using scanning probe microscope equipped with Nanoscope IV controller (Veeco Metrology Group, USA). The particle size distribution was analyzed by Mastersizer S nanoseries (Mulvern Instruments, Worcestershire, UK).

Chemical synthesis (Scheme 1)

Synthesis of p-alkoxycinnamic acids

p-(2-hydroxy-ethoxy) cinnamic acid (**M2**) was prepared by refluxing a solution of *p*-hydroxycinnamic acid (0.01 mol) in acetonitrile (50 mL) with 2-bromoethanol in the presence of potassium carbonate (0.10 mol). The reaction was quenched by removing the heat and filtering out potassium carbonate. Then, saturated sodium bicarbonate (30 mL) was added to the filtrant and the mixture was extracted with dichloromethane (2 × 20 mL) to remove excess bromo alkyl alcohol. The aqueous layer was slowly poured into a beaker containing cold 40% hydrochloric acid (20 mL) and the white solid (*p*-(2-hydroxy

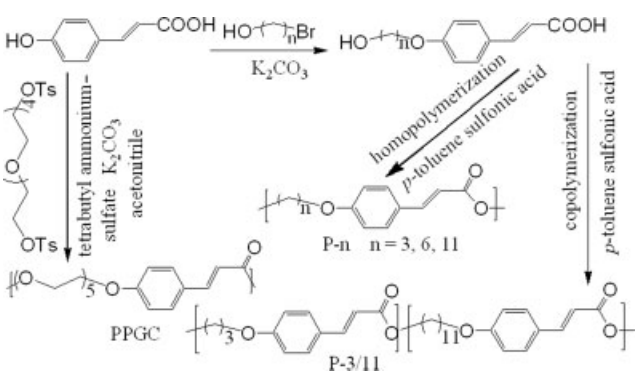

Scheme 1 Chemical synthesis of the monomers and the oligomers.

ethoxy) cinnamic acid) was separated by suction filtration, washed with cold water and dichloromethane.

p-(3-Hydroxy-propoxy) cinnamic acid (**M3**), *p*-(6-hydroxy-hexyloxy) cinnamic acid (**M6**) and *p*-(11-hydroxy-undecyloxy) cinnamic acid (**M11**) were prepared using a similar procedure. Corresponding bromo alkyl alcohol was used in place of 2-bromoethanol and hexane was used to extract 11-bromo-1-undecanol during the acid-base extraction procedure.

p-(2-Hydroxy-ethoxy) cinnamic acid (M2). White solid; yeild: 73%. m.p.: 193.5–195.5°C. Retention factor or R_f: 0.31 (SiO_2, EtOAc/hexane, 70 : 30). ^{1}H NMR (400 MHz, $CDCl_3$, δ, ppm): 7.70 (d, J = 16.6 Hz, 1H, Ar—C**H**=), 7.50 (d, J = 8.6 Hz, 2H, Ar—**H**), 6.94 (d, J = 8.5 Hz, 2H, Ar—**H**), 6.32 (d, J = 15.3 Hz, 1H, = C**H**—COOH), 4.13 (t, 2H, —C**H$_2$**—O—Ar), 3.99 (t, 2H, HO—C**H$_2$**). ^{13}C NMR (100 MHz, DMSO-d_6, δ, ppm): 168.4 (—**C**OOH), 144.3 (Ar—**C**H=), 160.9 (—O—Ar), 130.4 (2 × 1C), 127.2 (Ar—CH), 115.3 (2 × 1C) (aromatic carbons), 116.9 (=**C**H—COOH), 70.1 (—**C**H$_2$—O—Ar), 60.1 (HO—**C**H$_2$—). IR (KBr, cm^{-1}): 3387–2580, 1676, 1599, 1245. MS (*m/z*): calcd for $C_{11}H_{12}O_4$, 208; found, 207 [M-H]$^-$.

p-(3-Hydroxy-propoxy) cinnamic acid (M3). White solid; yeild: 97%. m.p.: 152.0–154.0°C. R_f 0.31 (SiO_2, EtOAc/hexane, 70 : 30). ^{1}H NMR (400 MHz, $CDCl_3$, δ, ppm): 7.71 (d, J = 16.6 Hz, 1H, Ar—C**H**=), 7.49 (d, J = 8.6 Hz, 2H, Ar—**H**), 6.92 (d, J = 8.6 Hz, 2H, Ar—**H**), 6.31 (d, J = 16.5 Hz, 1H, = C**H**—COOH), 4.16 (t, 2H, —C**H$_2$**—O—Ar), 3.88 (t, 2H, HO—C**H$_2$**). ^{13}C NMR (100 MHz,DMSO-d_6, δ, ppm): 168.3 (—**C**OOH), 144.2 (Ar—**C**H=), 160.8 (—O—Ar), 130.4 (2 × 1C), 127.1 (Ar—CH), 115.2 (2 × 1C) (aromatic carbons), 116.8 (=**C**H—COOH), 65.2 (—**C**H$_2$—O—Ar), 57.6 (HO—**C**H$_2$—) and 32.4 (—**C**H$_2$—). IR (KBr, cm^{-1}): 3420–2362, 1676, 1603, and 1247. MS (*m/z*): calcd for $C_{12}H_{14}O_4$, 222; found, 221 [M-H]$^-$.

p-(6-Hydroxy-hexyloxy) cinnamic acid (M6). White solid; yield: 69%. m.p.: 162–165°C. R_f: 0.36 (SiO_2, EtOAc/hexane, 70 : 30). ^{1}H NMR (400 MHz, $CDCl_3$, δ, ppm): 7.70 (d, J = 15.5 Hz, 1H, Ar—C**H**=), 7.48 (d, J = 7.9 Hz, 2H, Ar—**H**), 6.90 (d, J = 7.8 Hz, 2H, Ar—**H**), 6.30 (d, J = 17.4 Hz, 1H,=C**H**—COOH), 3.99 (t, 2H, —C**H$_2$**—O—Ar), 3.66 (t, 2H, HO—C**H$_2$**). ^{13}C NMR (100 MHz, DMSO-d_6, δ, ppm): 168.0 (—**C**OOH), 144.0 (Ar—**C**H=), 130.4 (2 × 1C), 160.8 (—O—Ar), 127.1 (Ar—CH), 115.2 (2 × 1C) (aromatic carbons), 116.8 (=**C**H—COOH), 68.0 (—**C**H$_2$—O—Ar), 61.1 (HO—**C**H$_2$—), 32.90, 29.08, and 25.82 (alkyl carbons). IR (KBr, cm^{-1}): 3250–2547, 1668, 1603, and 1247. MS (*m/z*): calcd for $C_{15}H_{20}O_4$, 264; found, 263 [M-H]$^-$.

p-(11-Hydroxy-undecyloxy) cinnamic acid (M11). White solid; Yield: 89%. m.p.: 128.0–130.0°C. R_f: 0.39 (SiO_2, EtOAc/hexane, 70 : 30). ^{1}H NMR (400 MHz, $CDCl_3$, δ, ppm): 7.71 (d, J = 15.8 Hz, 1H, Ar—C**H**=), 7.48 (d, J = 8.46 Hz, 2H, Ar—**H**), 6.90 (d, J = 8.56 Hz, 2H, Ar—**H**), 6.31 (d, J = 15.71 Hz, 1H,=C**H**—COOH), 3.99 (t, 2H, —C**H$_2$**—O—Ar), 3.64 (t, 2H, HOvC**H$_2$**). ^{13}C NMR (100 MHz, DMSO-d_6, δ, ppm): 168.3 (—**C**OOH), 144.2 (Ar—**C**H=), 160.8 (—O—Ar), 130.3 (2 × 1C), 127.1 (Ar—CH), 115.2 (2 × 1C) (aromatic carbons), 116.8 (=CH—COOH), 68.0 (—**C**H$_2$—O—Ar), 61.2 (HO—**C**H$_2$—), 33.0, 29.4, and 26.0 (alkyl carbons). IR (KBr, cm^{-1}): 3396–2567, 1683, 1606, and 1280. MS (*m/z*): calcd for $C_{20}H_{30}O_4$, 334; found, 333 [M-H]$^-$.

Poly(p-propoxycinnamate) (P3), poly(p-hexyloxycinnamate) (P6), and poly(p-undecyloxycinnamate) (P11)

A monomer (0.50 g) and *p*-toluene sulfonic acid (0.10 g, 20% w/w) were refluxed in 30 mL toluene. The reaction mixture was quenched by cooling and filtering through No.1 Whatman filter paper. The filtrate was evaporated, dissolved in 25 mL dichloromethane, washed with saturated sodium bicarbonate solution (3 × 20 mL), dehydrated with anhydrous sodium sulfate and the solvent was removed by a rotary evaporator.

Low molecular weight poly (p-undecyloxycinnamate) (P11a)

To carry out polymerization of **M11** at a more diluted concentration of the monomer, a similar polymerization reaction as described above was carried out for only 24 h. After 24 h, 250 mL of toluene was added into the reaction mixture and the mixture was refluxed for another 48 h. The reaction was then quenched by cooling and filtering. The filtrate was dried and then redissolved in 25 mL dichloromethane. The obtained solution was washed with saturated sodium bicarbonate solution (3 × 50 mL), dehydrated with anhydrous sodium sulfate and the solvent was removed by rotary evaporator.

Poly(p-propoxycinnamate) (P3). Pale brown solid; T_g: 50.7°C. Melting temperature or T_m: 154.2 PC. $\overline{M_n}$: 2000. ^{1}H NMR (400 MHz, $CDCl_3$, δ, ppm): 7.80–6.15 (br, Ar—**H**, Ar—C**H**=, =C**H**—COO—), 4.46–3.50 (br, —C**H$_2$**—O—Ar, —COO—C**H$_2$**—) and 2.48–1.86 (br, —C**H$_2$**—). IR (KBr, cm^{-1}): 3427, 2958, 1708, 1604, and 1251.

Poly(p-hexyloxycinnamate) (P6). Pale brown solid; $\overline{M_n}$: 3000. ^{1}H NMR (400 MHz, $CDCl_3$, δ, ppm): 7.69–6.10 (br, Ar—**H**, Ar—C**H**=,=C**H**—COO—), 4.24–3.29 (br, —C**H$_2$**—O—Ar, —COO—C**H$_2$**—) and 2.44–1.12 (br, —C**H$_2$**—). IR (KBr, cm^{-1}): 3403, 2939, 1709, 1605, and 1290.

Poly(p-undecyloxycinnamate) (P11). Pale brown solid; T_g: 53.4°C. $\overline{M_n}$: 5500. ^{1}H NMR (400 MHz, $CDCl_3$, δ, ppm): 7.67–6.25 (br, Ar—**H**, Ar—C**H**=, =C**H**—

COO—), 4.24–3.60 (br, —C**H**$_2$—O—Ar, —COO—C**H**$_2$—) and 1.83–1.15 (br, —C**H**$_2$—). IR (KBr, cm^{-1}): 3423, 2977, 1709, 1604, and 1252.

Poly(p-undecyloxycinnamate) ***(P11a).*** Pale yellow solid; T_g: 50.5°C. $\overline{M_n}$: 2500. ^{1}H NMR (400 MHz, $CDCl_3$, δ, ppm): 7.56 (d, J = 15.6 Hz, 1H, Ar—C**H**=), 7.38 (t, 2H, Ar—**H**), 6.80 (t, 2H, Ar—**H**), 6.23 (d, J = 16.3 Hz, 1H, =C**H**—COOH), 4.12, 3.86, and 3.56 (t, 2H, —C**H**$_2$—O—Ar and —COO—C**H**$_2$—). IR (KBr, cm^{-1}): 3431, 2926, 1708, 1605, and 1297.

Poly(p-ethoxycinnamate) (P2). Monomer **M2** (0.20 g, 1 × 10^{-3} mole) and *N*,*N*′-dicyclohexylcarbodiimide, DCC (0.20 g, 1 × 10^{-3} mole) were refluxed in 15 mL acetone. After 24 h, the white solid (*N*,*N*′-dicyclohexylurea, DCU) was removed by filtration. The filtrate was evaporated, dissolved in 30 mL dichloromethane and left for several days to precipitate out additional DCU. The solution was then filtered and washed with water (2 × 25 mL), dehydrated with anhydrous sodium sulfate and the solvent was removed by rotary evaporation.

Poly(p-ethoxy cinnamate) ***(P2).*** Orange solid; ^{1}H NMR (400 MHz, $CDCl_3$, δ, ppm): 7.89–6.40 (br, Ar—**H**, Ar—C**H**=, =C**H**—COO—), 4.13, 4.00, and 3.78 (br, —O—C**H**$_2$—, —C**H**$_2$—O—Ar and —COO—C**H**$_2$—). IR (KBr, cm^{-1}): 3000–3300, 2932, 1704, 1647, and 1211–1130.

Poly(*p*-propoxycinnamate)-co-(*p*-undecyloxycinnamate) (P3/11)

M3 (0.25 g), **M11** (0.09 g), and *p*-toluene sulfonic acid (0.10 g, 20% w/w) were refluxed in 30 mL toluene. During the 72 h of the reflux, two batches of 0.08 g **M11** were added to the reaction mixture at hours 12 and 24 of the reaction. The reaction was quenched by removal from the heat and filtering through No.1 Whatman paper. The filtrate was evaporated, dissolved in 30 mL dichloromethane, washed with saturated sodium bicarbonate solution (3 × 25 mL), dehydrated with anhydrous sodium sulfate, and dried by rotary evaporation, to obtain **P3/11**. The insoluble part from the reaction mixture was washed with water prior to IR analysis.

Poly(p-propoxycinnamate)-co-(p-undecyloxycinnamate) ***(P3/11).*** Pale brown solid; $\overline{M_n}$: 2000. ^{1}H NMR (400 MHz, $CDCl_3$, δ, ppm): 7.75–6.09 (br, Ar—**H**, Ar—C**H**=, =C**H**—COO—), 4.40–3.44(br, —C**H**$_2$—O—Ar, —COO—C**H**$_2$—) and 2.17–1.10 (br, —C**H**$_2$—). IR (KBr, cm^{-1}): 3409, 2927, 1688, 1605, and 1252.

Poly(penta ethylene glycol cinnamate)

In the 50-mL two-neck round bottom flask, *p*-hydroxycinnamic acid (0.16 g, 1 × 10^{-3} mole) was dissolved in 10 mL of acetonitrile and potassium carbonate (1.38 g, 1 × 10^{-2} mole), after which tetrabutyl ammonium sulfate (0.04 g, 20% w/w) and pentaethylene glycol ditosylate (1.09 g, 2 × 10^{-3} mole) were added. The mixture was refluxed and the reaction was quenched by cooling to room temperature. The solvent was then removed and the product was dissolved in 25 mL ethyl acetate, washed with water (3 × 20 mL), dehydrated with anhydrous sodium sulfate and dried by rotary evaporation.

Poly(pentaethylene glycol cinnamate) ***(PPGC).*** Yellowish oil; T_m: 202.1°C. $\overline{M_n}$: 3000. ^{1}H NMR (400 MHz, $CDCl_3$, δ, ppm): 7.62 (d, J = 16.1 Hz, 1H, Ar—C**H**=), 7.43 (d, J = 8.16 Hz, 2H, Ar—**H**), 6.88 (d, J = 7.8 Hz, 2H, Ar—**H**), 6.31 (d, J = 15.5 Hz, 1H, =C**H**—COOH), 4.32 (br, —COO—C**H**$_2$—CH$_2$—O), 4.25 (br, —CH$_2$—C**H**$_2$—O—), 4.12 (br, —CH$_2$—C**H**$_2$—O—Ar), 3.86–3.54 (br, —C**H**$_2$—O—Ar). ^{13}C NMR (100 MHz, $CDCl_3$, δ, ppm): 167.2 (—**C**OO—), 144.7 (Ar—**C**H=), 160.6 (—O—Ar), 129.7 (2 × 1C), 127.2 (Ar—CH), 114.9 (2 × 1C) (aromatic carbons), 115.3 (=**C**H—COO) and 72.7–61.6 (—O—**C**H$_2$—). IR (Nujol, cm^{-1}): 2955, 2856, 1707, 1603, and 1258.

UV absorption and photostability test

Solution containing the exact amount of the test material was freshly prepared and UV absorption spectrum was then acquired. The molar absorption coefficient of each compound was obtained from the slope of the graph between molar concentrations and absorbances (at maximum absorption wavelength).

The photostability tests were performed in dichloromethane and methanol. The freshly prepared test solutions were divided into two parts. One part was kept in a light-proof condition at room temperature (dark sample) while the other part (irradiated sample) was irradiated with 0.50 mW/cm^2 UVB at the same temperature for 5, 10, 15, 20, 25, 30, 40, 50, and 60 min, which correspond to UVB exposures of 0.15, 0.30, 0.45, 0.60, 0.75, 0.90, 1.2, 1.5, and 1.8 J, respectively. Next, the UV absorption profile of each sample was acquired using a UV/VIS spectrometer. The absorbances of the irradiated samples at various irradiant times were reported as relative percentages to the absorbance of the dark sample.

Transdermal penetration

Transdermal penetration of **P3**, **P6**, **P11**, PPGC, and EHMC across the abdominal skin of a two-week-old baby mouse (*Mus musculus Linn*.) was carried out as described previously using a Franz diffusion cell with a 13.0 mL capacity receptor compartment and 2.27 cm^2 diffusion area.[20] In short, the experiment was initiated by dropping 200 μL of the 0.17 mol of cinnamate unit/L sample solution into the upper

compartment of the diffusion cell, directly onto the mounted skin (UV filter final coverage = 1.5×10^{-5} mol of the cinnamate unit/cm^2). Then, at 1, 2, 4, and 24 h, 3.4 mL of receptor fluid was withdrawn and replaced with a fresh receptor medium. Experiments were performed at room temperature in five repetitions. Since the skins from different mice were different, the penetration of each sunscreen sample was compared to the penetration of EHMC using the skin from the same mouse. Analysis of the withdrawn fluid were done using UV absorption spectroscopy. A sample solution was prepared by dissolving the tested material in DMSO to give the final concentration of 0.17 mol of cinnamate unit/L.

Nanoparticulate formation

PPGC was induced into nanoparticulates using solvent displacement technique (dialysis method). Twenty milligrams of PPGC were dissolved in 5 mL of DMF/DMSO (3 : 2) and this solution was dialyzed against deionized water (Milli-Q®). After dialysis, a colloidal suspension of nanoparticles in water was obtained in the dialysis bag. Final volume of the suspension was adjusted to 10 mL with water to obtain the suspension at 2 mg/mL. Similar procedure was carried out with **P3**, **P6**, and **P11**.

RESULTS AND DISCUSSION

Successful preparation of *p*-alkoxycinnamic acid could be achieved from a substitution reaction between *p*-hydroxycinnamic acid and bromo alkyl alcohol using potassium carbonate to generate nucleophiles from *p*-hydroxycinnamic acid (pK_a of the phenolic proton $\cong$10 (Scheme 1)). Excess bromo alkyl alcohol was used to maximize the yield of this S_N1 reaction (Table I). After completing the reaction, excess bromo alkyl alcohol could be recovered from the reaction mixture by solvent extraction.

All four *p*-alkoxycinnamic acids, *p*-(2-hydroxy ethoxy) cinnamic acid (**M2**), *p*-(3-hydroxy-propoxy) cinnamic acid (**M3**), *p*-(6-hydroxy-hexyloxy) cinnamic acid (**M6**), and *p*-(11-hydroxy-undecyloxy) cinnamic acid (**M11**) showed a similar UVB absorption of $\sim$26,000M^{-1} cm^{-1} (λ_{max} of 310 nm) in methanol. Similar UV absorption spectra among the four monomers corresponded well to the same UV-absorptive functionality among the four monomers.

Three monomers, **M3**, **M6**, and **M11** were successfully condensation polymerized by an esterification reaction using *p*-toluene sulfonic acid as a catalyst (Scheme 1). ^{1}H NMR and IR spectra, together with molecular weight information from GPC, indicated that esterifications had been taking place for **M3**, **M6**, and **M11** yielding poly(*p*-propoxy cinnamate) (**P3**), poly(*p*-hexyloxy) cinnamate) (**P6**) and poly(*p*-undecyloxy cinnamate) (**P11**), respectively. Both insoluble products (solid product precipitated out from the reaction medium) and soluble oligomeric products (soluble in the reaction medium) of **P3**, **P6**, and **P11** were obtained in the reaction mixtures. In all three cases, both soluble and insoluble products gave similar IR spectra, indicating that the insoluble products possessed similar functionalities to the soluble products. It was observed that polymerization at higher monomer concentration yielded more insoluble solid product. The phase separation of the larger insoluble oligomers from the reaction mixture resulted in a dilution of the remaining soluble oligomers in the reaction mixture. It was speculated that such dilution might favor cyclization of the soluble oligomeric molecules. The soluble oligomers, therefore, stopped increasing their sizes. The small cyclized product was found by mass spectrometry. MALDI-TOF MS spectra gave m/z = 612 and 816 for **P3**, m/z = 738 and 984 for **P6** and m/z = 632 and 948 for **P11**. It should be noted here that the lack of peak at higher m/z in the mass spectra is probably a result of undesorbable nature of the bigger species. Esterification was also verified by the differences in the positions of —OCH_2— resonances between the monomers' and oligomers' ^{1}H NMR spectra [see details in the ^{1}H NMR information in the experimental section and Fig. 1(a,b)]. The lack of broad absorption band around 2300–3600 cm^{-1} (—COOH) in the FTIR spectra of **P3**, **P6**, and **P11** together with the shift of carbonyl stretching from $\sim$1670 cm^{-1} in the IR spectra of monomers to $\sim$1710 cm^{-1} in the spectra of the oligomers also confirmed the complete condensations (Fig. 2). GPC analysis of the final soluble products gave $\overline{M_n}$ values for **P3**, **P6**, and **P11** of $\sim$1600, 3500, and 5500, respectively. It can

TABLE I
Reaction Conditions for the Synthesis of the Monomers

Monomer	n	Mole equivalent of bromo alkyl alcohol	Reaction time (h)	% yield
p-(2-hydroxy-ethoxy) cinnamic acid (**M2**)	2	10	36	73
p-(3-hydroxy-propoxy) cinnamic acid (**M3**)	3	5	27	97
p-(6-hydroxy-hexyloxy) cinnamic acid (**M6**)	6	3	40	69
p-(11-hydroxy-undecyloxy) cinnamic acid (**M11**)	11	3	40	89

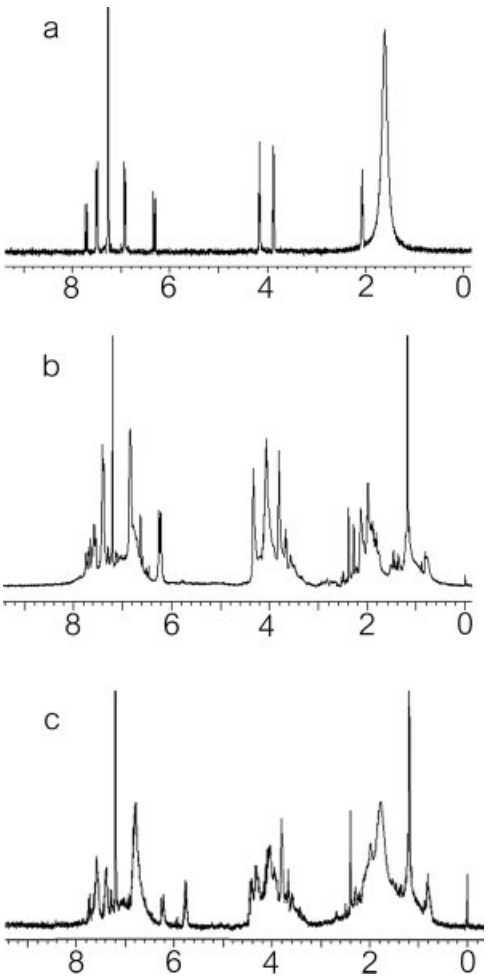

Figure 1 ^{1}H NMR spectra of (a) *p*-(3-hydroxy-propoxy) cinnamic acid (**M3**), (b) poly(*p*-propoxycinnamate) (**P3**), and (c) **P3** after being exposed to 1.80 J of UVB.

be seen from the growth curves of **P3** and **P6** that the maximum $\overline{M_n}$ values for the two oligomers to stay soluble in the reaction medium, are probably 2500 and 4000, respectively, (Fig. 3). The decrease in the $\overline{M_n}$ value of the soluble **P6** after the oligomers' size reached 4500 was probably caused by precipitation of those oligomers with $\overline{M_n}$ values over 4000. This situation can also be seen in **P3**. However, in the case of **P11**, a smooth growth curve was observed. This can be explained by the fact that **P11** possesses a better solubility in the reaction medium than **P3** and **P6**.

Since **P3**, **P6**, and **P11** were polymerized at a similar molar concentration of the monomers, it can be concluded that the hydrocarbon chain length in the oligomeric structure directly affects the solubility of the compound. We speculated that the polymerization reaction carried out at a more diluted monomer concentration should yield more soluble oligomeric product with a smaller $\overline{M_n}$ value, and significantly less insoluble product. The experiment showed that polymerization under lower concentration of **M11** gave **P11a** ($\overline{M_n}$ 2500) with no solid precipitate.

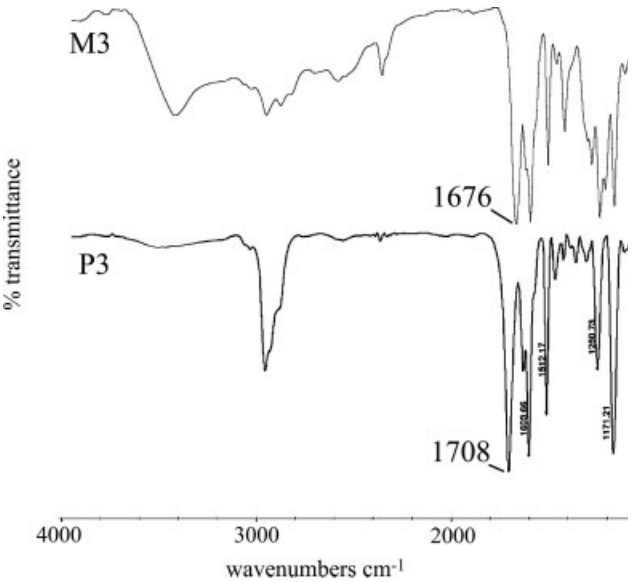

Figure 2 FTIR spectra of M3 (top) and P3 (bottom). M3 spectrum shows stretching of the carbonyl from carboxylic acid fuctionality at 1676 cm^{-1}, while P3 spectrum shows stretching from ester carbonyl at 1708 cm^{-1}.

It should be noted here that polymerization of **M2** using either *p*-toluene sulfonic acid, Amberlyst-15 (cationic ion-exchange resin) or 1-(3-dimethylamino-propyl)-3-ethylcarbodiimide hydrochloride (EDCI) plus 1-hydroxy-benzotriazole (HOBt) failed. Only the use of *N*,*N*′-dicyclohexylcarbodiimide (DCC) as coupling agent gave poly(*p*-(2-ethoxy)cinnamate), **P2**. ^{1}H NMR analysis indicated a little contamination of *N*,*N*′-dicyclohexylurea (DCU).

Copolymerization of **M3** and **M11** was successfully carried out using *p*-toluene sulfonic acid (Scheme 1). Since it was previously observed that **M11** could be polymerized more easily than **M3**, the copolymerization was performed by starting with

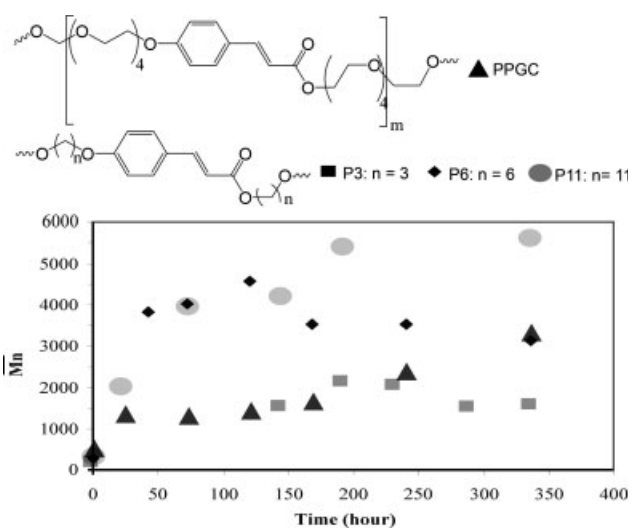

Figure 3 $\overline{M_n}$ of the soluble oligomers in the reaction mixtures at various reaction times.

TABLE II
Solubility of P3, P6, P11, P11a, P3/11, and PPGC

Solvent	**P3** ($\overline{Mn}$ = 2000)	**P6** ($\overline{Mn}$ = 3000)	**P11** ($\overline{Mn}$ = 5500)	**P11a** ($\overline{Mn}$ = 2500)	**P3/11** ($\overline{Mn}$ = 2000)	**PPGC** ($\overline{Mn}$ = 3000)
Water	−−	−−	−−	−−	−−	−−
Acetonitrile	+−[a]	+−[a]	+−[a]	+−[a]	+−	++
Ethanol	+−[a]	+−[a]	+−[a]	+−[a]	+−[a]	+−[a]
Methanol	+−[a]	+−[a]	+−[a]	+−[a]	+−[a]	+−[a]
Acetone	++[a]	++[a]	++[a]	++[a]	++	+−
Ethyl acetate	++	++[a]	++[a]	++[a]	++	+−
Tetrahydrofuran	++	++	++	++	++	++
Chloroform	++	++	++	++	++	++
Dichlorometane	++	++	++	++	++	++
Diethyl ether	+−	++	++	++	++	−−
Toluene	++	++	++	++	++	−−
Hexane	−−	−−	−−	−−	−−	−−
DC200[b]	−−	−−	−−	−−	−−	++
DC556[c]	−−	−−	−−	−−	−−	++

−− less than 2 mg/mL; +− 2–10 mg/mL; ++ more than 20 mg/mL.
[a] After heated.
[b] Linear polydimethylsiloxane polymers.
[c] Phenyl trimethicone.

more **M3** than **M11**. Additional amounts of **M11** were added at later times during the reaction. At the conclusion of the polymerization, the moles of the two monomers were equal. The resulting poly(*p*-propoxy cinnamate)-*co*-(*p*-undecyloxy cinnamate) or **P3/11** ($\overline{M_n}$ 2000) shows a better solubility than **P3** ($\overline{M_n}$ 1600) and **P11** ($\overline{M_n}$ 5500) (see Table II), i.e., **P3/11** is soluble in acetone at 25°C, while both **P3** and **P11** are soluble in hot acetone (reflux). This is likely a result of a random alteration between the *p*-propoxy cinnamoyl and the *p*-undecyloxy cinnamoyl units, which results in less stacking among cinnamoyl moieties.

Copolymerization between one mole equivalent of *p*-hydroxycinnamic acid and two mole equivalents of pentaethylene glycol ditosylate in acetonitrile using potassium carbonate as a catalyst and tetrabutylammonium sulfate as a phase transferring agent, yielded poly(penta ethylene glycol cinnamate) or PPGC (Scheme 1) as a liquid product. Partitioning between ethyl acetate and water removed the polyethylene glycol from the product. It can be clearly seen that polymerization occurred steadily and the chain growth continued, even after reaction times of 2 weeks (Fig. 3). This steady growth was a result of an excellent solubility of the growing polymer chains. The outstanding characteristic of PPGC is that it is a light-yellow-oily liquid, miscible with silicone fluids used in the cosmetic industry (see Table II).

P2, **P3**, **P6**, **P11**, **P3/11**, and PPGC showed similar UVB absorption characteristics (Fig. 4). This is expected because all five oligomers contain similar chromophore (cinnamate moiety). It should be noted here that the molar absorption coefficients of all oligomers were calculated per mole of the cinnamate unit. This should permit the direct comparison in UVB absorption efficiency of cinnamate moieties of different compounds.

Photostability study of the commonly used UVB filter 2-ethylhexyl-*p*-methoxycinnamate (EHMC), **P3**, **P6**, **P11**, **P3/11**, and PPGC in dichloromethane indicated comparable photostability among the five oligomers and EHMC (Fig. 5). NMR analysis indicated *trans* to *cis* photoisomerization of the cinnamate moieties in all five oligomers and also in EHMC (decrease of resonance at 6.2 ppm (d, J = 16.0 Hz, 1H, *trans* CH=C**H**—COO) and appearance of resonance at 5.8 ppm (d, J = 8.0 Hz, 1H, *cis* CH=C**H**—COO), see Figure 1(b,c). The isomerization into the *cis* configuration, which possesses less molar absorption coefficient than that of the *trans*,[23,24] lowers the absorption efficiency of the oligomer. It should be noted here, however, that there was no other degradation product found during the photostability test. This indicated that all the oligomers could still act as UV absorbers during their UV exposures but with lower UV absorption efficiency.

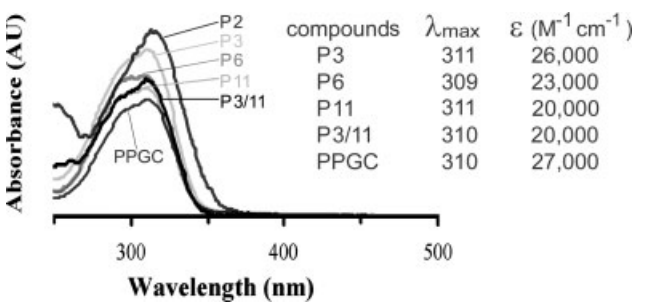

Figure 4 UV Absorption characteristics of the synthesized oligomers. The molar absorption coefficients (ε) were obtained from the slopes of the graphs between concentrations of the oligomers and the absorbances. The concentrations of the oligomers used were based on the molar concentrations of cinnamoyl monomeric units. Molar absorption coefficients are expressed based on molar concentration of cinnamoyl monomeric units.

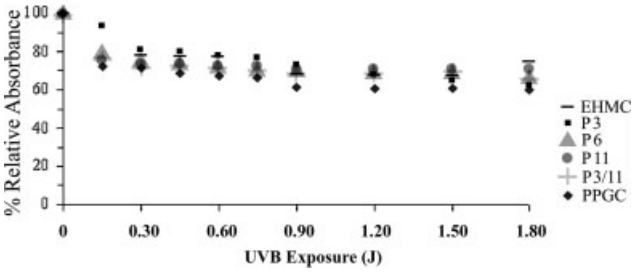

Figure 5 Photostability of each synthesized oligomer comparing with EHMC. The photostability was expressed as % relative absorbance of the material after being exposed to various UVB doses, as compared to the absorbance of the unexposed material.

P3, **P6**, **P11**, **P3/11**, and PPGC showed no transdermal penetration across baby mouse skin, while EHMC showed obvious penetration (Fig. 6). In the experiment, coverages of the materials on the skin were reported as cinnamate unit per cm^2. The experiments were carried out at similar cinnamate unit/cm^2 for all oligomers and EHMC, therefore, coverages of the chromophoric units (cinnamate units) on the skin were similar among different samples. This transdermal penetration of EHMC agrees well with previous study.[25] The nonpenetrating nature of the oligomers is likely a result of the bulky oligomeric structure of the materials. This nonpenetrating nature of the compounds should prolong the UV-absorption efficiency of the compound when being applied onto the skin. The water immiscibility and liquid nature of PPGC also encourage further study for application of the compound in cosmetics.

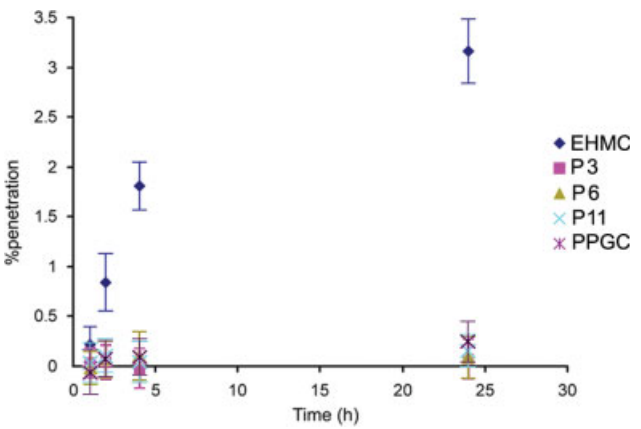

Figure 6 Penetration of the synthesized oligomers and EHMC through baby mouse skins using Franz diffusion cells with the skin contact area of 0.175 cm^2/mL and at the final coverage of UV filter on the baby mouse skin of 4.4 mg/cm^2. The results are shown as percentages of UV filters found in receptor fluid as relating to the amount of applied UV filters, at various post application times. The data are shown as average values of at least three experimental repetitions. Maximum standard deviation was 0.9%. [Color figure can be viewed in the online issue, which is available at www.interscience.wiley.com.]

Since PPGC is amphiphilic, there was a possibility that the compound could be formed into micelles. Self-assembly of the PPGC at the concentration of 0.40 (w/v) using solvent displacement (dialysis) technique, gave aqueous colloidal suspensions with mean hydrodynamic diameters of micelles from dynamic light scattering of ~164 nm (dispersity index, DPI, = 0.142) [Fig. 7(a)]. Scanning electron micrograph (SEM) at 20,000× magnification of PPGC-micelles revealed semispherical shape [Fig. 7(b)]. It should be noted here that it was very difficult to get the SEM picture of PPGC particles since most particles either melted or burst during the gold deposition process and during the impact of the high energy-electrons. One of the two particles shown in Figure 7(b), was in the middle of such burst. In facts, many of such bursts were observed during the SEM acquisition for the PPGC particles. Atomic force micrograph (AFM) of the PPGC particles also indicated soft semispherical particles [Fig. 7(c)]. At room temperature, PPGC colloidal suspension was stable and showed no precipitation even after being kept for 6 months. A self-assembly of amphiphilic polymer, although, is quite common,[26–28] the self-assembled amphiphilic PPGC-nanoparticles reported here is unique as the PPGC is UV-absorptive material by itself. In other words, organic UV absorptive nanoparticles were synthesized in this work. Further studies on the use of such particles as cosmetic active carrier, for an additional benefit on UV protection of the encapsulated materials, are currently being carried out in our laboratory.

P3, **P6**, and **P11** which contain no hydrophilic PEG moieties, were also subjected to dialysis process to

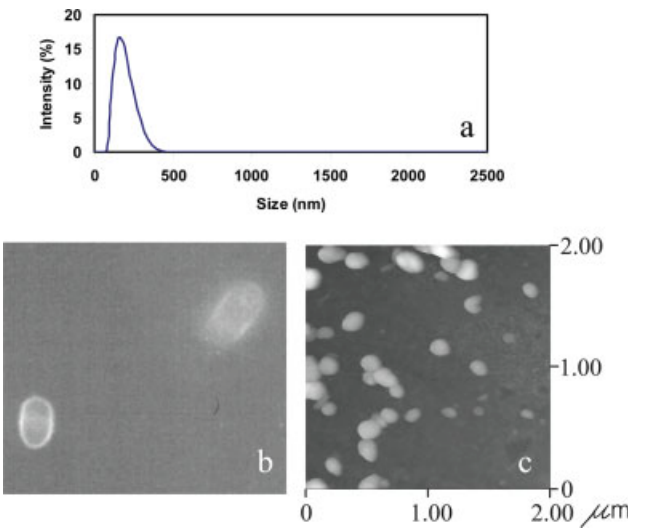

Figure 7 Size distribution of PPGC aqueous suspension prepared at 0.4% (w/v) of PPGC (top) and SEM of PPGC particles obtained at 20,000× magnification (bottom). [Color figure can be viewed in the online issue, which is available at www.interscience.wiley.com.]

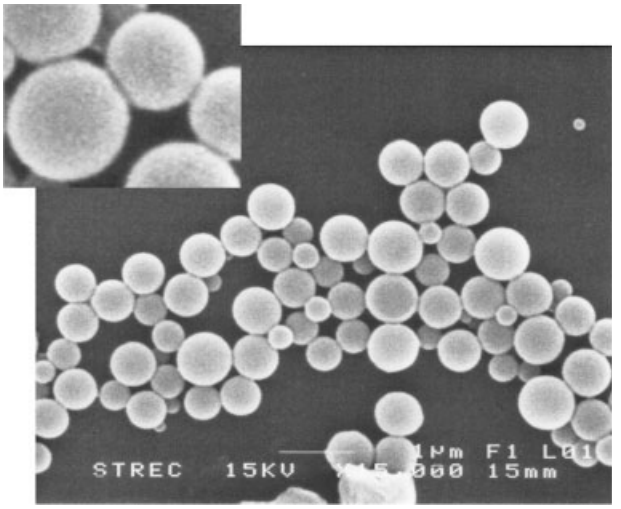

Figure 8 Scanning Electron Micrograph (SEM) of **P3** particles.

induce self-assembly into particles. Only **P3** yielded colloidal suspension of spherical particles (Fig. 8). The **P3** colloidal suspension agglomerated and precipitated quickly. Association among **P3** particles could be observed clearly (see inset of Fig. 8). The fact that the **P3** particles did not disperse well in water while the PPGC particles could form stable colloidal suspension in water, indicates an importance of a big hydrophilic segment (PEG moiety) in PPGC structure. Since **P6** and **P11** were even more hydrophobic than **P3**, it was not surprised to observe that both oligomers did not give colloidal suspension after dialysis.

CONCLUSIONS

Three solid UV-absorptive oligomers—poly(*p*-propoxycinnamate) (**P3,** $\overline{M_n}$ 2000), poly(*p*-hexyloxycinnamate) (**P6,** $\overline{M_n}$ 3000), and poly(*p*-undecyloxycinnamate) (**P11,** $\overline{M_n}$ 5500 and **P11a**, $\overline{M_n}$ 2500)—were successfully condensation polymerized from *p*-(3-hydroxy-propoxy) cinnamic acid, *p*-(6-hydroxy-hexyloxy) cinnamic acid and *p*-(11-hydroxy-undecyloxy) cinnamic acid, respectively. Copolymerization between *p*-(3-hydroxy-propoxy) cinnamic acid and *p*-(11-hydroxy-undecyloxy) cinnamic acid yielded poly (*p*-propoxycinnamate)-co-(*p*-undecyloxycinnamate) (**P3/11**, $\overline{M_n}$ 2000). The liquid UV-absorptive oligomer, poly(pentaethylene glycol cinnamate) (PPGC, $\overline{M_n}$ 3000), was synthesized through the copolymerization between *p*-hydroxycinnamic acid and pentaethylene glycol ditosylate. Absorption profiles of all synthesized polymers indicated UVB absorption characteristics. Upon UVB exposure, all synthesized oligomers and the standard UVB filter, 2-ethylhexyl-*p*-methoxycinnamate (EHMC), underwent *trans* to *cis* photoisomerization at the cinnamoyl moieties which resulted in the decrease in UVB absorption efficiency of the materials. However, no transdermal penetration across a baby mouse skin (*Mus musculus* Linn.) was detected for all the synthesized oligomers, while the penetration of EHMC through the same skin was clearly observed. In addition, poly(pentaethylene glycol cinnamate), a yellowish water immiscible liquid, showed good solubility in various organic solvents and silicone fluids. Using solvent displacement technique, the amphiphilic PPGC oligomer could be induced into nanoparticles with the hydrodynamic size of ~164 nm (DPI = 0.142). These particles formed stable colloidal suspension in water.

References

1. Gallagher, R. P.; Lee, T. K. Prog Biophys Mol Biol 2006, 92, 119.
2. Daya-Grosjean, L.; Dumaz, N.; Sarasin, A. J Photochem Photobiol B 1995, 28, 115.
3. Taylor, J. S.; Lu, H. F.; Kotyk, J. J Photochem Photobiol 1990, 51, 161.
4. Ziegler, A.; Leffell, D. J.; Kunala, S.; Sharma, H. W.; Gailani, M.; Simon, J. A.; Halperin, A. J.; Baden, H. P.; Shapiro, P. E.; Bale, A. E. Proc Nat Acad Sci USA 1993, 90, 4216.
5. Kielbassa, C.; Roza, L.; Epe, B. Carcinogenesis 1997, 18, 811.
6. Courdavault, S.; Baudouin, C.; Charveron, M.; Canguilhem, B.; Favier, A.; Cadet, J.; Douki, T. DNA Repair 2005, 4, 836.
7. Kimura, K.; Katoh, T. Contact Dermat 1995, 32, 304.
8. Schauder, S.; Ippen, H. Contact Dermat 1997, 37, 221.
9. Hany, J.; Nagel, R. Deutsche Lebensmittel-Rundschau 1995, 91, 341.
10. Janjua, N. R.; Mogensen, B.; Andersson, A. M.; Petersen, J. H.; Henriksen, M.; Skakkebaek, N. E.; Wulf, H. C. J Invest Dermatol 2004, 123, 57.
11. Jiang, R.; Roberts, M. S.; Collins, D. M.; Benson, H. A. E. Brit J Clin Pharmaco 1999, 48, 635.
12. Hayden, C. G. J.; Roberts, M. S.; Benson, H. A. E. Lancet 1997, 350, 863.
13. Yener, G.; Incegul, T.; Yener, N. Int J Pharm 2003, 258, 203.
14. Calderilla-Fajardo, S. B.; Cazares-Delgadillo, J.; Villalobos-Garcia, R.; Quintanar-Guerrero, D.; Ganem-Quintanar, A.; Robles, R. Drug Dev Ind Pharm 2006, 32, 107.
15. Chatelain, E.; Gabard, B.; Surber, C. Skin Pharmacol Appl Skin Physiol 2003, 16, 28.
16. Kamiya, H.; Kita, K.; Fijikura, Y. Jpn. Pat. 7,173,027 (1995).
17. Pattanaargson, S.; Hongchinnagorn, N.; Hirunsupachot, P.; Sritana-anant, Y. Photochem Photobiol 2004, 80, 322.
18. Vaughan-Spickers, J.; Greenfield, S.; Hassall I. V. E.; Dunn, C. J.; Harding, R.; Jenkins, T.; May, A. L. U.S. Pat. 26,660 (2004).
19. Harding, R.; Hassall I. V. E.; Maren, S. A.; Brown, D. U.S. Pat. 7,294,369 (2007).
20. Richard, H.; Ledue, M. U.S. Pat. 6,080,880 (2000).
21. Ledue, M.; Richard, H.; Lagrange, A. U.S. Pat. 6,376,679B2 (2002).
22. Langer, M. E.; Khorshahi, F. U.S. Pat. 5,250,652 (1993).
23. Pattanaargson, S.; Limphong, P. Int J Cosmet Sci 2001, 23, 151.
24. Pattanaargson, S.; Munhapol, T.; Hirunsupachot, P.; Luangthongaram, P. J Photochem Photobiol 2004, 161, 269.
25. Klinubol, P.; Asawanonda, P.; Wanichwecharungruang, S. P. Skin Pharmacol Physiol 2008, 21, 23.
26. Letchford, K.; Burt, H. Eur J Pharm Biopharm 2007, 65, 259.
27. Chen, C.; Yu, C. H.; Cheng, Y. C.; Yu, P. H. F.; Cheung, M. K. Eur Polym Mater 2006, 42, 2211.
28. Kim, S. Y.; Shin, I. G.; Lee, Y. M. J Control Release 1998, 56, 197.